SUPPLEMENTARY MATERIAL

Monitoring Greenland ice-sheet buoyancy-driven calving discharge using glacial earthquakes

Amandine Sergeant[1,2], Anne Mangeney[2,3], Vladislav A. Yastrebov[4], Fabian Walter[1], Jean-Paul Montagner[2], Olivier Castelnau[5], Eléonore Stutzmann[2], Pauline Bonnet[2,4], Velotioana Jean-Luc Ralaiarisoa[2,6], Suzanne Bevan[7] and Adrian Luckman[7]

[1] Laboratory of Hydraulics, Hydrology and Glaciology, ETH Zürich, Zürich, Switzerland

[2] Institut de Physique du Globe de Paris, CNRS UMR 7154, Université Paris Diderot-Paris 7, Paris, France

[3] ANGE team, INRIA, Laboratoire Jacques-Louis Lions, Paris, France

[4] MINES ParisTech, PSL Research University, Centre des Matériaux, CNRS UMR 7633, Evry, France

[5] Processes and Engineering in Mechanics and Materials, CNRS UMR 8006, ENSAM, CNAM, Paris, France

[6] Now at Institut de Physique de Rennes, Université Rennes, CNRS UMR 6251, Rennes, France

[7] Geography Department, College of Science, Swansea University, SA2 8PP, United Kingdom

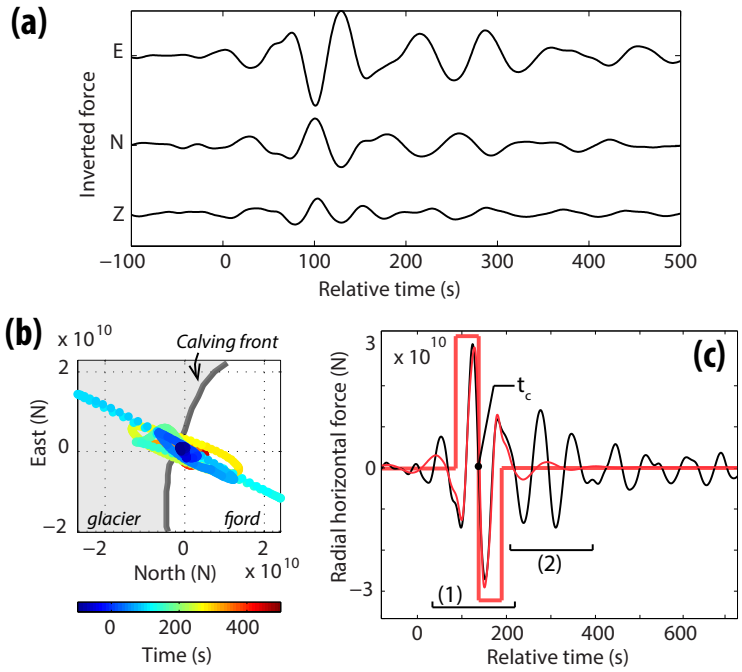

Figure S1: Polarization analysis of the force inverted from the 25 July 2013 glacial earthquake and force rotation in the radial horizontal direction, normal to the glacier calving front. Force time-series in the (a) East, North and vertical directions. (b) North force amplitudes as a function of the East force amplitudes. Color dots indicate the time. It shows the linear polarization of the glacial earthquake force that points normally to the Helheim glacier calving front (grey line) with azimuth of -64°. (c) Force time-series when rotated in its horizontal radial direction. Two phases can be defined. The first part of the force (1) can be described by a CSF model (thick red line) when filtered in the seismic band 0.01-0.05 Hz (red dashed line). We note t_c the centroid time for the CSF. This force (1) is associated to the capsizing iceberg-to-terminus contact according to *Sergeant et al.* (2016, 2018) and *Murray et al.* (2015). The latter part of the force (2) may be related to other post-calving seismic sources and are not discussed in this study.

Calving volume synthetic inversions: text related to Fig. S2 In order to assess the feasibility of the designed procedure to estimate iceberg volumes from the generated contact forces, we perform synthetic

inversions of the model parameters using force models as inputs, filtered in the period band 20-100 s of GEs. Two tests are designed.

First, we compare the magnitudes A_{CSF} of each pair of forces. We construct the misfit function $|(A_{CSF}(\epsilon_k, H_l) - A_{CSF_d})|$, with A_{CSF_d} the CSF magnitude of the input force model (ϵ_d, H_d) and $A_{CSF}(\epsilon_k, H_l)$ the magnitude of each force model for different iceberg ϵ and H. CSF magnitudes are computed by twice-integrating in time the CSF models which best reproduce filtered contact forces.

Results are shown in Figure S2a-b. Whereas minimum difference in A_{CSF} is achieved for correct input force model ($\epsilon_0 = \epsilon_d, H_0 = H_d$), very low misfit values (within the black dashed contour line) are yield for a wide and various range of iceberg aspect ratios and heights. Lower misfit ϵ and H values can then lead to large ambiguities in estimated iceberg volumes, when we invert for the contact force magnitude (or amplitude) only.

Best-fitting (ϵ, H) values are then calculated from the comparison of the force histories using the variance reduction (VR) of their misfit (Figure S2c-d). As for the first inversion with A_{CSF}, maximum VR values are achieved for correct iceberg dimensions ($\epsilon_0 = \epsilon_d, H_0 = H_d$) of the input forces. Nevertheless, the

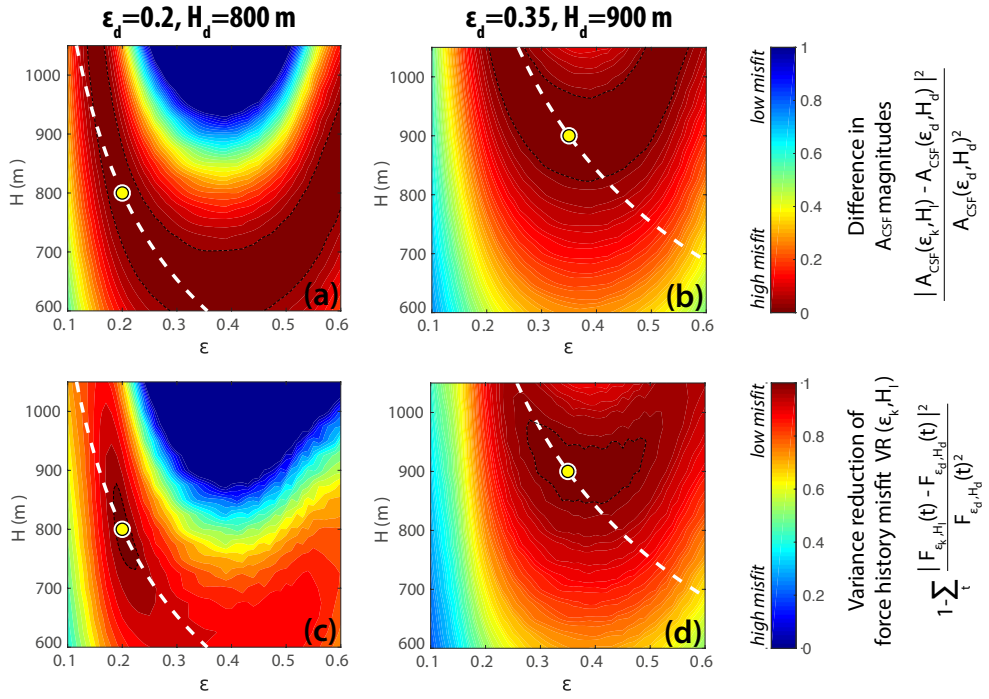

Figure S2: Synthetic inversion of force models when bandpass filtered in the seismic band (20-100 s). Misfit function variation with iceberg dimensions ϵ and H for two inversions of input force models that correspond to (a, c) $\epsilon_d = 0.2$ and $H_d = 800$ m, (b, d) $\epsilon_d = 0.35$ and $H_d = 900$ m. (a-b) correspond to the difference magnitudes A_{CSF} of every pair of forces. (c-d) correspond to the variance reduction (VR) measured for each pair of force times-series. The best-fitting parameters are indicated by yellow dots and correspond to actual dimensions of input models. The iceberg isovolume is indicated by the white dashed line. Black dashed contour lines indicate the confidence interval for the retrieved parameters (ϵ, H) that yield to misfit values greater that 98% of the best value that is minimum amplitude difference for (a-b) and maximum VR for (c-d). This Figure illustrates that the uncertainty on calculated best-fitting iceberg dimensions and then estimated volume is very high when comparing force amplitudes or magnitudes only, due to the symmetry of the contact force with respect to $\epsilon \sim 0.4$ (*Sergeant et al.*, 2018). Using the force history information enables to better constrain parameters, especially ϵ-values which primarily control the capsize dynamics, and then reduce iceberg volume ambiguities.

uncertainty on iceberg aspect ratio and height that is computed from (ϵ, H) values which lead to high VR (i.e. VR$\geq$98% of maximum VR) is considerably decreased and enable to constrain more precisely iceberg individual dimensions and volume.

An interesting observation is that lower misfit ϵ and H values are likely distributed in different regions depending on the choice of ϵ_0. For ϵ_0 close to 0.2 (Figure S2a-c), one can define two areas for lowest misfit, around $\epsilon \approx 0.2$ and $\epsilon \approx 0.5$ (dark red colors). These patterns essentially come from the variation of the contact force amplitudes with iceberg dimensions that are almost symmetrical with respect to $\epsilon \approx 0.4$ (*Sergeant et al.*, 2018). This symmetric distribution of contact force amplitudes then yield to larger uncertainty in retrieved (ϵ, H) values when the aspect ratio is close to 0.4 (Figure S2b-d).

Finally, despite high achieved VR values for each inversion set, the uncertainty on (ϵ, H) values come from the filtering of the contact forces within the GE seismic band ($\geq$ 100 s) which lead to distortion of force waveform and loss of information on the capsize dynamics and generated contact. The wider the frequency band used for the inversion is (i.e. toward lower frequencies), the less the force energy is depleted (*Sergeant et al.*, 2018). However, these synthetic inversion tests show the ability to retrieve correct model parameters and iceberg dimensions from the contact force when bandpass filtered in the recorded frequency range of GEs. Accounting for the force time variation rather than its amplitude only, enables to capture the iceberg capsize dynamics that are distinguishable among various iceberg geometries, even when filtered, and finally better constrain ϵ and H and reduce uncertainty on calving volumes.

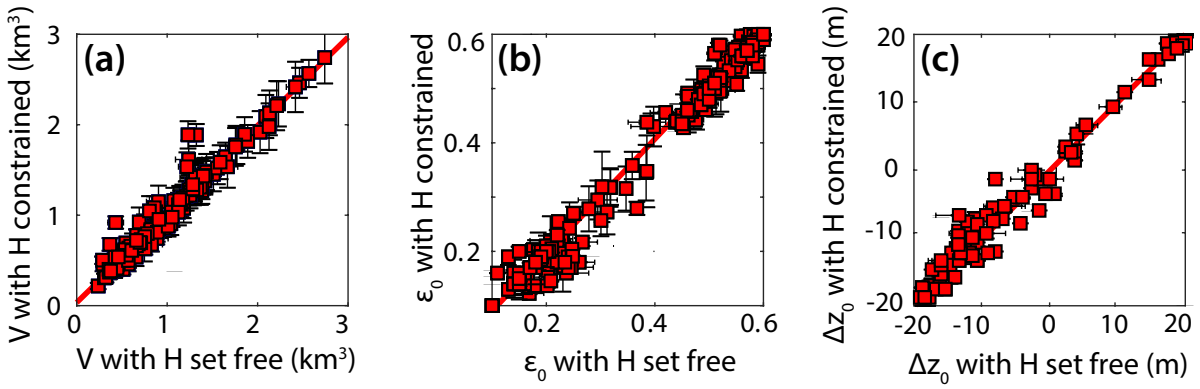

Figure S3: MCI result consistency for (a) the iceberg volumes V, (b) aspect ratio ϵ, and (c) parameter Δz, when the iceberg height H is constrained to $\pm$15% of the glacier thickness (y-axis) and when H is set free (x-axis) in the final calculation of V. Error bars indicate uncertainties as defined in equation 1 in the paper.

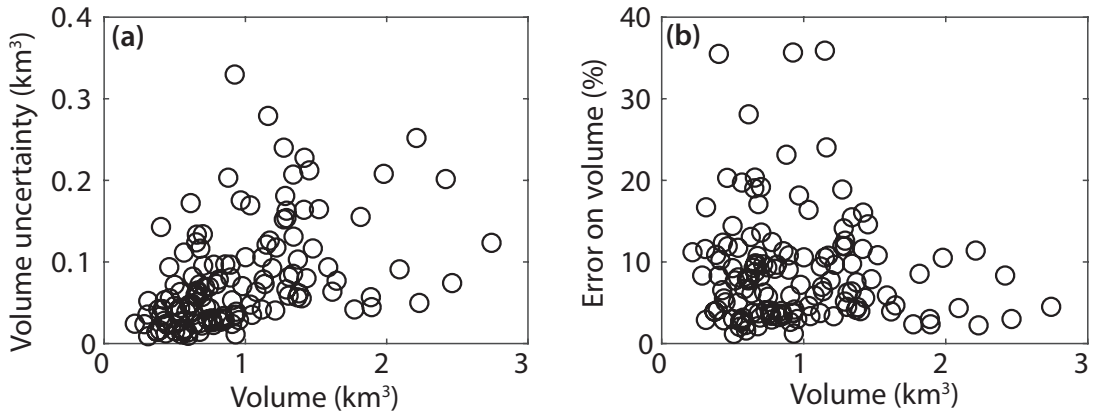

Figure S4: Uncertainty on calculated iceberg volumes in (a) km^3 and (b) in percentage of volumes.

References

Murray, T., M. Nettles, N. Selmes, L. Cathles, J. Burton, T. James, S. Edwards, I. Martin, T. O'Farrell, R. Aspey, et al. (2015), Reverse glacier motion during iceberg calving and the cause of glacial earthquakes., *Science (New York, NY)*.

Sergeant, A., A. Mangeney, E. Stutzmann, J.-P. Montagner, F. Walter, L. Moretti, and O. Castelnau (2016), Complex force history of a calving-generated glacial earthquake derived from broadband seismic inversion, *Geophysical Research Letters*, *43*(3), 1055–1065.

Sergeant, A., V. A. Yastrebov, A. Mangeney, O. Castelnau, J.-P. Montagner, and E. Stutzmann (2018), Numerical modeling of iceberg capsizing responsible for glacial earthquakes, *Journal of Geophysical Research: Earth surface*, doi: 10.1029/2018JF004768.